

Long-Range Influence of a Pump on a Critical Fluid

Ydan Ben Dor,¹ Yariv Kafri¹, David Mukamel², and Ari M. Turner¹

¹*Department of Physics, Technion—Israel Institute of Technology, Haifa 3200003, Israel*

²*Department of Physics of Complex Systems, Weizmann Institute of Science, Rehovot 7610001, Israel*



(Received 5 December 2021; accepted 30 March 2022; published 13 April 2022)

A pump coupled to a conserved density generates long-range modulations, resulting from the non-equilibrium nature of the dynamics. We study how these modulations are modified at the critical point where the system exhibits intrinsic long-range correlations. To do so, we consider a pump in a diffusive fluid, which is known to generate a density profile in the form of an electric dipole potential and a current in the form of a dipolar field above the critical point. We demonstrate that while the current retains its form at the critical point, the density profile changes drastically. At criticality, in $d < 4$ dimensions, the deviation of the density from the average is given by $\text{sgn}[\cos(\theta)] |\cos(\theta)/r^{(d-1)}|^{1/\delta}$ at large distance r from the pump and angle θ with respect to the pump's orientation. At short distances, there is a crossover to a $\cos(\theta)/r^{d-3+\eta}$ profile. Here δ and η are Ising critical exponents. The effect of the local pump on the domain wall structure below the critical point is also considered.

DOI: [10.1103/PhysRevLett.128.154501](https://doi.org/10.1103/PhysRevLett.128.154501)

Consider a fluid continuously pumped by a localized force. When the force couples to a conserved field, such as momentum or density, it leads to a nonlocal steady-state flow in the system. A canonical example arises when a localized force is exerted on an incompressible fluid at low Reynolds number. The resulting flow is long ranged, decaying as a power law with the distance from the pump [1,2]. The solution, known as a Stokeslet, is the Green's function of the Stokes equations. This solution plays an important role in the understanding of many phenomena. Examples include microswimmers [3–5], hydrodynamic interactions [6–9], and the large class of problems associated with slender-body motion [10–12]. In this case the force couples to the momentum flux, since it acts as a source of momentum.

A simpler case is that of a diffusive system where a localized pump drives the particles in a specific direction. Here momentum is not conserved, but the coupling of the pump to the conserved particle density results in long-range currents accompanied by density modulations due to the finite compressibility. In particular, it has been shown that in a hard core gas, corresponding to infinite temperature, the density profile induced by the pump is of the form of a dipole potential and the current is proportional to the gradient of the density [13,14].

The above results pertain to systems which without the pump have short range correlations. Here we ask what happens when the underlying fluid is critical, where one expects nontrivial interplay between the long-range correlations of the critical fluid and the long-range perturbation induced by the pump. Detailed analysis of this setup is, however, rather involved as it requires going beyond

deterministic hydrodynamics due to the large fluctuations and long-range correlations existing in this system.

In this Letter we make a first step towards addressing this problem by studying a pump in a critical diffusive system. This diffusive problem is directly relevant to interacting colloidal particles [15,16], which may be studied next to a surface where energy and momentum are not conserved. These can be pumped, for example, by using optical tweezers to bias the motion of colloids along a small segment in a specific direction [17–19].

To study the interplay between the nonlocal structure induced by the pump and critical correlations we consider a pump in an interacting dissipative system with density conservation, such as a lattice-gas system evolving by Kawasaki dynamics, which exhibits a liquid-gas phase transition. We show that above the critical temperature as well as at criticality and slightly below it, the current takes the form of a dipolar electric field. In contrast, the behavior of the density changes dramatically as a function of temperature. Above the critical temperature the behavior is qualitatively identical to that found in Refs. [13,14] for a hard core gas: At large distance r from the pump the density decays to the average density as $\cos(\theta)/r^{(d-1)}$, with θ the angle measured with respect to the direction of the driving force and $d > 1$ the dimension of the system. On the other hand, at the critical point the density develops a nontrivial scale-dependent behavior. In particular, in $d < 4$ dimensions the density exhibits a crossover from one scaling form to another at a distance r^* from the pump which varies as an inverse power of the drive. At distances $r < r^*$, the density profile takes the form $\cos(\theta)/r^{d-3+\eta}$, while for $r > r^*$, it becomes $\text{sgn}[\cos(\theta)] |\cos(\theta)/r^{(d-1)}|^{1/\delta}$, where η and δ are

the Ising exponents with $\eta = 1/4$ and $\delta = 15$ in $d = 2$ and $\eta \simeq 3.63 \times 10^{-2}$ and $\delta \simeq 4.79$ in $d = 3$. This implies that in $d = 2$ dimensions and at short distances the magnitude of the density modulation grows with r as $r^{3/4}$, and has a $\cos(\theta)$ angular dependence. On the contrary, in the far field the magnitude of the density modulation decays extremely slowly as a function of r , as $r^{-1/15}$. This is accompanied by a change in the angular dependence of the density profile into $\text{sgn}[\cos(\theta)]|\cos(\theta)|^{1/15}$. The crossover distance r^* between the two behaviors scales as $f^{-8/7}$, with f the strength of the pump. These results are compared with numerical simulation in Fig. 1, where we use a magnetic Ising system corresponding to a lattice gas, so that $s_i = \pm 1$, the magnetization at site i , is related to the density through $n_i = (1 + s_i)/2$. The pump locally swaps two pairs of spins [20], such that for each pair $s_L = +1$ on the left and $s_R = -1$ on the right become $s_L = -1$ and $s_R = +1$. A three-dimensional version of Fig. 1 can be found in the Supplemental Material [20]. Finally, we also study the system below the critical temperature and show that the pump controls the shape and location of the domain wall between the two phases. This is illustrated for zero average magnetization in Fig. 1. While in the low temperature phase

our theoretical arguments hold only in the vicinity of the critical point, they qualitatively agree with the numerics also at lower temperatures.

To obtain these results it is useful to consider a localized pump acting on an Ising lattice gas with a conserved magnetization field, $\phi(\mathbf{r})$, representing the local deviation of the density from the overall average density. Hereafter we simply refer to $\phi(\mathbf{r})$ as the local density. The Landau-Ginzburg free energy of the gas is given by

$$\mathcal{F}_0 = \int d^d r \left[\frac{K}{2} |\nabla \phi|^2 + \frac{\tau}{2} \phi^2 + \frac{u}{4} \phi^4 \right], \quad (1)$$

with $K, u > 0$, and $\tau \propto (T - T_c)/T_c$. The model evolves by the magnetization-conserving model B dynamics

$$\begin{aligned} \partial_t \phi &= -\nabla \cdot \mathbf{J}, \\ \mathbf{J} &= \mathbf{J}_0 + \mathbf{\Lambda} + M \mathbf{f} \delta^{(d)}(\mathbf{r}), \end{aligned} \quad (2)$$

where $\mathbf{J}(\mathbf{r})$ is the current. Here \mathbf{J}_0 is the usual deterministic part of the current,

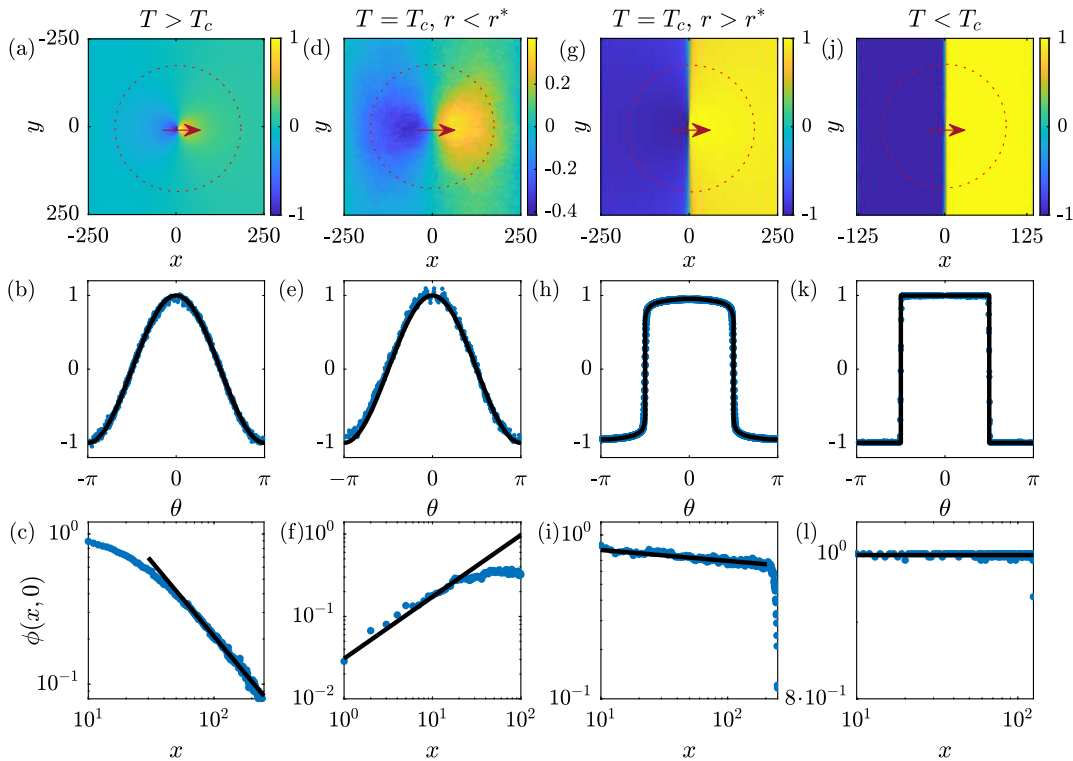


FIG. 1. Results for a two-dimensional $L \times L$ lattice gas with zero magnetization in the presence of a pump (indicated by an arrow) above ($T = 4.54J$), at ($T = 2.27J$), and below ($T = 1.14J$) criticality. The top row [(a),(d),(g),(j)] shows magnetization profiles, the middle row [(b),(e),(h),(k)] the measured angular dependence of the density at $r = 0.35L$ (on the dotted circles in the top row) compared to the theoretical prediction [black line, Eqs. (9), (18), and (14)], and the bottom row [(c),(f),(i),(l)] the radial dependence of the magnetization along the direction of the pump, as a function the distance from it compared to the theoretical prediction [black line, Eqs. (9), (18), and (14)]. At the critical point we consider two pump strengths allowing us to verify the behavior below and above r^* . For $T > T_c$ and $T = T_c$, $L = 512$ while for $T < T_c$, $L = 256$.

$$\mathbf{J}_0 = -M\nabla\mu[\phi] = -M\nabla\frac{\delta\mathcal{F}_0}{\delta\phi}, \quad (3)$$

with $\mu[\phi]$ the chemical potential. The Gaussian white noise term, $\Lambda(\mathbf{r}, t)$, has zero mean with a variance satisfying $\langle\Lambda_i(\mathbf{r}, t)\Lambda_j(\mathbf{r}', t')\rangle = 2D\delta_{ij}\delta^{(d)}(\mathbf{r} - \mathbf{r}')\delta(t - t')$, where the angular brackets denote an average over histories. The pump, of fixed strength \mathbf{f} , localized at the origin, is accounted for by the last term in Eq. (2). It is represented by a delta function, which yields the correct behavior in the far field for any localized drive. Finally, $D = MT$ with T the temperature, and M is the mobility. In general M depends on the magnetization ϕ . In what follows we consider the case of ϕ -independent mobility. This is valid above and in the vicinity of the critical point where the coarse-grained magnetization is small, so that a small ϕ expansion can be applied. Implications of magnetization-dependent mobility are discussed later.

We first consider the current. To do so we use density conservation; because of the constant mobility the steady-state average of the chemical potential satisfies Poisson's equation

$$\nabla^2\langle\mu\rangle = \nabla \cdot [\mathbf{f}\delta^{(d)}(\mathbf{r})]. \quad (4)$$

This implies that $\langle\mu\rangle = (1/S_d)(\mathbf{f} \cdot \mathbf{r}/r^d)$ with $S_d = 2\pi^{(d/2)}/\Gamma(d/2)$ the area of a d -dimensional unit sphere and Γ is the Gamma function. Hence the average steady-state current takes the form of the field of an electric dipole:

$$\langle\mathbf{J}\rangle(\mathbf{r}) = -M\nabla\langle\mu\rangle = \frac{M}{S_d} \frac{1}{r^d} \left[\frac{d(\mathbf{f} \cdot \mathbf{r})\mathbf{r}}{r^2} - \mathbf{f} \right]. \quad (5)$$

This motivates us, following existing literature, to refer to \mathbf{f} as the dipole strength. This result is confirmed numerically in Fig. 3 of the Supplemental Material [20].

Before proceeding to the analysis of the density profile in the various temperature regimes we note that while the system is *out of equilibrium*, its steady-state properties such as the density profile may be obtained by studying an equivalent *equilibrium* system. This observation is found useful in the analysis that follows and in the numerical studies of the model. To see this, we use a Helmholtz-Hodge decomposition

$$\mathbf{f}\delta^{(d)}(\mathbf{r}) = \nabla h_{\text{eff}} + \boldsymbol{\zeta}, \quad (6)$$

where h_{eff} is a scalar function and $\boldsymbol{\zeta}$ satisfies $\nabla \cdot \boldsymbol{\zeta} = 0$. Using this in Eq. (2) shows that the density profile is only affected by ∇h_{eff} . The statistics of ϕ are then described by an *equilibrium* problem with the free energy

$$\mathcal{F} = \mathcal{F}_0 - \int d^d x h_{\text{eff}} \phi, \quad (7)$$

with \mathcal{F}_0 given in Eq. (1) and h_{eff} accounting for the pump. Taking the divergence of Eq. (6), one finds that

$$h_{\text{eff}}(\mathbf{r}) = \frac{1}{S_d} \frac{\mathbf{f} \cdot \mathbf{r}}{r^d}, \quad (8)$$

is *nonlocal*, decaying as a power law.

The equivalence between the equilibrium and nonequilibrium models for the density is verified numerically in Figs. 4–5 of the Supplemental Material [20]. There we compare conserving, nonequilibrium Kawasaki dynamics for a lattice gas with nonconserving, equilibrium Wolff cluster dynamics [21,22] for the density. The Wolff cluster algorithm is much more efficient than the conserving Kawasaki dynamics, as it avoids critical slowing down. This allows us to present results for large systems. In Fig. 1 we present results of the Wolff algorithm above and at the critical point for two-dimensional periodic lattices of size 512×512 . Below the critical point, where the mapping to the equilibrium problem is not expected to hold due to the dependence of the mobility on the magnetization, we present results using Kawasaki dynamics for the non-equilibrium model with smaller systems. We now turn to the analysis of the magnetization profiles.

A pump above the critical temperature.—Above the critical temperature, namely, for $\tau > 0$, where the correlation length is finite, one may ignore the $K|\nabla\phi|^2$ term in Eq. (1) on length scales larger than the correlation length. In addition, far from the pump, h_{eff} is small so the nonlinear term in Eq. (1) may be ignored as well. Minimizing the free energy (7) yields

$$\langle\phi\rangle \sim \frac{1}{S_d\tau} \frac{\mathbf{f} \cdot \mathbf{r}}{r^d}. \quad (9)$$

This density profile is verified numerically in the leftmost column of Fig. 1. For self-consistency it is straightforward to verify that the terms in \mathcal{F}_0 ignored in the derivation make negligibly small contribution to Eq. (9) at large distances. This result has previously been obtained in Refs. [13,14] for a lattice gas model of hard core diffusing particles, corresponding to infinite temperature.

As τ is lowered to approach the critical point the derivation of Eq. (9) becomes invalid, as manifested by the divergence of the expression of the density profile. This is due to the diverging susceptibility $\chi \propto \tau^{-1}$ (or compressibility of the lattice gas) which is linked to the diverging correlation length.

A pump in a critical system.—We start with a mean-field calculation, valid for $d > d_c = 4$. To this end, we minimize \mathcal{F} , the effective free energy (7), to obtain

$$0 = K\nabla^2\phi_{\text{MF}} - u\phi_{\text{MF}}^3 + \frac{1}{S_d} \frac{\mathbf{f} \cdot \mathbf{r}}{r^d}, \quad (10)$$

where we set $\tau = 0$. In the far field we expect the nonlinear contribution to be negligible, leading to

$$\phi_{\text{MF}} \propto \mathbf{f} \cdot \mathbf{r} / K r^{d-2}. \quad (11)$$

Note that this decays slower than the $\tau > 0$ solution Eq. (9), but retains the same angular dependence. The self-consistency of the solution can be checked by comparing the contributions of the nonlinear and linear terms in Eq. (10). One finds that $u\phi_{\text{MF}}^3 \ll K\nabla^2\phi_{\text{MF}}$ on distances larger than $r^* \propto [uf^2/K^3]^{1/[2(d-4)]}$, where $f = |\mathbf{f}|$. This distance is finite for any dipole strength \mathbf{f} in $d > 4$ and thus at large distance Eq. (11) holds.

Next, we consider the behavior for $d < 4$. As the results above show, the density modulations in this pumped critical system are described by an equilibrium model with a magnetic field $h_{\text{eff}}(\mathbf{r})$ which decays as a power law with the distance from the pump. Note that in general the presence of a magnetic field h induces a finite correlation length, $\xi(h)$. To derive $\xi(h)$ we use the equation of state $\phi \sim h^{1/\delta}$ with h small, along with the linear-response relation

$$\frac{\partial\phi}{\partial h} = \beta \int d\mathbf{r} G(\mathbf{r}, h), \quad (12)$$

where β is the inverse temperature. One finds

$$\xi(h) \sim h^{-\frac{(\delta-1)}{\delta(2-\eta)}}. \quad (13)$$

Here $G(\mathbf{r}, h) = \xi^{-(d-2+\eta)} g(r/\xi)$ is the connected magnetization correlation function and η the anomalous exponent associated with the correlation length.

Returning to the problem of a space-dependent magnetic field h_{eff} , we reason that if in a certain region the field varies on scales much larger than $\xi(h_{\text{eff}})$ the system should behave locally as if it is subject to a constant field h_{eff} . Using the equation of state $\phi \sim h_{\text{eff}}^{1/\delta}$ with Eq. (8) for h_{eff} one finds

$$\phi^{\text{nonlin}} \propto \text{sgn}(\mathbf{f} \cdot \mathbf{r}) \left| \frac{\mathbf{f} \cdot \mathbf{r}}{r^d} \right|^{1/\delta}. \quad (14)$$

The condition for this to be valid is that $r \gg \xi(h_{\text{eff}})$, which using Eqs. (13) and (8) gives

$$r > r^* \sim f^{\frac{\delta-1}{d(\delta-1)-\delta(3-\eta)+1}}. \quad (15)$$

Using the scaling relation $2 - \eta = d(\delta - 1)/(\delta + 1)$ then gives $r^* \sim f^{-(\delta+1)/((\delta+1)-d)}$. In $d = 4 - \epsilon$ dimensions $\delta = 3 + \epsilon$ so that the leading order behavior of r^* is

$$r^* \sim f^{-2/\epsilon}, \quad (16)$$

which *diverges* as $f \rightarrow 0$. Using $\delta = 15$ and $\delta \simeq 4.79$ in $d = 2$ and $d = 3$, respectively, [23,24] one finds $r^* \sim f^{-8/7}$

and $r^* \sim f^{-2.08}$, respectively. It is interesting to note that this behavior is different than the one in $d > 4$ where the r^* decreases with f .

All in all we find that the far-field behavior below $d = 4$ is very different from that found for $d > 4$. In particular, the density profile is found to decay with the distance in the far field as $r^{-0.4}$ and $r^{-1/15}$ in $d = 3$ and $d = 2$ respectively. Furthermore, the angular dependence is also substantially modified. It is given by $\text{sgn}[\cos(\theta)]|\cos(\theta)|^{0.2}$ and $\text{sgn}[\cos(\theta)]|\cos(\theta)|^{1/15}$ for $d = 3$ and $d = 2$, respectively.

The fact that r^* increases with decreasing f implies that it is also of interest to study the behavior at distances $r < r^*$. Here the field h_{eff} changes much faster than $\xi(h_{\text{eff}})$ so that the previous treatment is not self-consistent. Then one can use perturbation theory to understand how the field influences the system. This gives

$$\phi^{\text{lin}} \equiv \langle \phi(\mathbf{r}) \rangle = \int d\mathbf{r}' G_0(\mathbf{r} - \mathbf{r}') h_{\text{eff}}(\mathbf{r}'), \quad (17)$$

where $G_0(\mathbf{r}) \propto 1/r^{d-2+\eta}$ is the renormalized Green's function, so that

$$\phi^{\text{lin}} \propto \frac{\mathbf{f} \cdot \mathbf{r}}{r^{d-2+\eta}}. \quad (18)$$

Note that the dipolar form of h_{eff} ensures that the integral Eq. (17) converges. This is the behavior one might expect naively from Eq. (11) when extended to include the fluctuations below d_c . The self-consistency of the linear-response approach can be checked by demanding that the fluctuations in the magnetization are larger than the mean induced magnetization. This justifies the use of the critical Green's function. Since the fluctuations of the magnetization on a scale r are given by $r^{-(d-2+\eta)/2}$ and the mean magnetization is given by Eq. (18) one finds that the approach breaks down on a scale $r^* \sim f^{2/(d-4+\eta)}$. This coincides with the scale at which the far-field behavior starts to work, see Eq. (15). Also, note that the two expressions $\phi^{\text{lin}}(\mathbf{r})$ and $\phi^{\text{nonlin}}(\mathbf{r})$ match at r^* .

Interestingly, for dimensions such that $d + \eta < 3$, i.e., two dimensions, the magnitude of the near-field density profile for $r < r^*$ is an *increasing* function of r . The results at the critical point are verified numerically in Figs. 1(d)–1(i) for a lattice gas in $d = 2$.

In Sec. V of the Supplemental Material [20] we also consider the richer behavior that arises close to but not exactly at criticality, due to the competition between the off-critical correlation length and the one induced by the magnetic field.

A pump below the critical temperature.—Here we take $\tau < 0$ where in the absence of a pump the system phase separates. Consider first the case studied above where the net magnetization in the system is zero. The magnetization is that of an equilibrium system with an effective magnetic

field given by Eq. (8) which changes sign on the plane $\mathbf{f} \cdot \mathbf{r} = 0$. Since $\tau < 0$, even a small field induces a large magnetization so that this plane divides the system between positive and negative magnetization regions. The two domains are separated by a narrow domain wall whose width is controlled by the correlation length of the system. The location and orientation of the domain wall is dictated by the pump. In addition, the magnetization is essentially constant in the bulk of the phases because the effective magnetic field is small. In Sec. IV of the Supplemental Material [20] we generalize the treatment to finite periodic systems with the dipole parallel to one of the periodic axes and to arbitrary values of the magnetization. In the latter case curved or closed domain walls appear.

Far below the critical point the local average magnetization becomes large and the magnetization dependence of the mobility is expected to modify our results. In particular, the mapping to an equilibrium model fails. Nonetheless, we show in Figs. 3 and 5 of the Supplemental Material [20] that our theory gives a qualitatively correct picture both for the magnetization and the current when compared to numerical simulations.

In summary, we studied the behavior of a pump in a conserving lattice gas, or its equivalent magnetic system at various temperatures. The most interesting behavior is found at the critical point, where there is an interplay between the long-range effects generated by the drive and the long-range critical correlations in the system. The problem studied opens the door to a host of questions. For example, it would be interesting to generalize this problem to fluids belonging to other dynamic and static universality classes, in particular to momentum-conserving ones. These might be realized experimentally using setups similar to that of Ref. [25]. In addition, it would be interesting to explore these questions in active systems where it is known that asymmetric objects placed in the fluid act as pumps even in the absence of external forces [26–29]. The closest system to the one considered above is dry scalar matter which has a critical point associated with a motility induced phase separation [30–35]. Our method might be used as a possible probe of the universality class of the system, a topic which has been under some debate [36–40].

We thank Tal Agranov, Anna Frishman, Omer Granek, Asaf Miron, and Sunghan Ro for helpful discussions. The work was supported by a research grant from the Center for Scientific Excellence at the Weizmann Institute of Science. Y.B.D. and Y.K. are supported by an Israel Science Foundation Grant No. 2038/21 and an NSF-BSF Grant No. 2016624. A. M. T. is supported by an Israel Science Foundation Grant No. 1939/18.

[1] G. G. Stokes, On the effect of the internal friction of fluids on the motion of pendulums, *Trans. Cambridge Philos. Soc.* **IX**, 8 (1851).

- [2] C. K. Batchelor and G. Batchelor, *An Introduction to Fluid Dynamics* (Cambridge University Press, Cambridge, England, 2000).
- [3] J. Elgeti, R. G. Winkler, and G. Gompper, Physics of microswimmers single particle motion and collective behavior: A review, *Rep. Prog. Phys.* **78**, 056601 (2015).
- [4] C. Bechinger, R. Di Leonardo, H. Löwen, C. Reichhardt, G. Volpe, and G. Volpe, Active particles in complex and crowded environments, *Rev. Mod. Phys.* **88**, 045006 (2016).
- [5] Ž. Kos and M. Ravnik, Elementary flow field profiles of micro-swimmers in weakly anisotropic nematic fluids: Stokeslet, stresslet, rotlet and source flows, *Fluids* **3**, 15 (2018).
- [6] H. Brenner, Hydrodynamic resistance of particles at small reynolds numbers, in *Advances in Chemical Engineering* (Elsevier, New York, 1966), Vol. 6, pp. 287–438.
- [7] S. Kim and S. J. Karrila, *Microhydrodynamics: Principles and Selected Applications* (Butterworth-Heinemann, Boston, 2013).
- [8] E. R. Dufresne, T. M. Squires, M. P. Brenner, and D. G. Grier, Hydrodynamic Coupling of Two Brownian Spheres to a Planar Surface, *Phys. Rev. Lett.* **85**, 3317 (2000).
- [9] T. Goldfriend, H. Diamant, and T. A. Witten, Hydrodynamic interactions between two forced objects of arbitrary shape. I. Effect on alignment, *Phys. Fluids* **27**, 123303 (2015).
- [10] G. Batchelor, Slender-body theory for particles of arbitrary cross-section in Stokes flow, *J. Fluid Mech.* **44**, 419 (1970).
- [11] R. E. Johnson, An improved slender-body theory for Stokes flow, *J. Fluid Mech.* **99**, 411 (1980).
- [12] I. Tanasijević and E. Lauga, Hydrodynamic interactions between a point force and a slender filament, *Phys. Rev. Fluids* **6**, 124101 (2021).
- [13] T. Sadhu, S. N. Majumdar, and D. Mukamel, Long-range steady state density profiles induced by localized drive, *Phys. Rev. E* **84**, 051136 (2011).
- [14] T. Sadhu, S. N. Majumdar, and D. Mukamel, Long-range correlations in a locally driven exclusion process, *Phys. Rev. E* **90**, 012109 (2014).
- [15] S. Faber, Z. Hu, G. H. Wegdam, P. Schall *et al.*, Controlling colloidal phase transitions with critical Casimir forces, *Nat. Commun.* **4**, 1584 (2013).
- [16] A. Maciołek and S. Dietrich, Collective behavior of colloids due to critical Casimir interactions, *Rev. Mod. Phys.* **90**, 045001 (2018).
- [17] Y. Roichman, V. Wong, and D. G. Grier, Colloidal transport through optical tweezer arrays, *Phys. Rev. E* **75**, 011407 (2007).
- [18] Y. Roichman, B. Sun, A. Stolarski, and D. G. Grier, Influence of Nonconservative Optical Forces on the Dynamics of Optically Trapped Colloidal Spheres: The Fountain of Probability, *Phys. Rev. Lett.* **101**, 128301 (2008).
- [19] H. Nagar and Y. Roichman, Collective excitations of hydrodynamically coupled driven colloidal particles, *Phys. Rev. E* **90**, 042302 (2014).
- [20] See Supplemental Material at <http://link.aps.org/supplemental/10.1103/PhysRevLett.128.154501> for detailed numerics, finite size effects, and an analysis just below the critical point.
- [21] U. Wolff, Lattice Field Theory as a Percolation Process, *Phys. Rev. Lett.* **60**, 1461 (1988).

- [22] J. Kent-Dobias and J. P. Sethna, Cluster representations and the Wolff algorithm in arbitrary external fields, *Phys. Rev. E* **98**, 063306 (2018).
- [23] M. Kardar, *Statistical Physics of Fields* (Cambridge University Press, Cambridge, England, 2007).
- [24] A. Pelissetto and E. Vicari, Critical phenomena and renormalization-group theory, *Phys. Rep.* **368**, 549 (2002).
- [25] I. Buttinoni, G. Volpe, F. Kümmer, G. Volpe, and C. Bechinger, Active Brownian motion tunable by light, *J. Phys. Condens. Matter* **24**, 284129 (2012).
- [26] P. Galajda, J. Keymer, P. Chaikin, and R. Austin, A wall of funnels concentrates swimming bacteria, *J. Bacteriol.* **189**, 8704 (2007).
- [27] A. Guidobaldi, Y. Jeyaram, I. Berdakin, V. V. Moshchalkov, C. A. Condat, V. I. Marconi, L. Giojalas, and A. V. Silhanek, Geometrical guidance and trapping transition of human sperm cells, *Phys. Rev. E* **89**, 032720 (2014).
- [28] Y. Baek, A. P. Solon, X. Xu, N. Nikola, and Y. Kafri, Generic long-range interactions between passive bodies in an active fluid, *Phys. Rev. Lett.* **120**, 058002 (2018).
- [29] O. Granek, Y. Baek, Y. Kafri, and A. P. Solon, Bodies in an interacting active fluid: Far-field influence of a single body and interaction between two bodies, *J. Stat. Mech.* (2020) 063211.
- [30] M. E. Cates and J. Tailleur, Motility-induced phase separation, *Annu. Rev. Condens. Matter Phys.* **6**, 219 (2015).
- [31] M. E. Cates and J. Tailleur, When are active Brownian particles and run-and-tumble particles equivalent? Consequences for motility-induced phase separation, *Europhys. Lett.* **101**, 20010 (2013).
- [32] J. Tailleur and M. E. Cates, Statistical Mechanics of Interacting Run-and-Tumble Bacteria, *Phys. Rev. Lett.* **100**, 218103 (2008).
- [33] I. Buttinoni, J. Bialke, F. Kummel, H. Lowen, C. Bechinger, and T. Speck, Dynamical Clustering and Phase Separation in Suspensions of Self-Propelled Colloidal Particles, *Phys. Rev. Lett.* **110**, 238301 (2013).
- [34] G. S. Redner, M. F. Hagan, and A. Baskaran, Structure and Dynamics of a Phase-Separating Active Colloidal Fluid, *Phys. Rev. Lett.* **110**, 055701 (2013).
- [35] S. Paliwal, J. Rodenburg, R. van Roij, and M. Dijkstra, Chemical potential in active systems: Predicting phase equilibrium from bulk equations of state?, *New J. Phys.* **20**, 015003 (2018).
- [36] F. Caballero, C. Nardini, and M. E. Cates, From bulk to microphase separation in scalar active matter: A perturbative renormalization group analysis, *J. Stat. Mech.* (2018) 123208.
- [37] B. Partridge and C. F. Lee, Critical Motility-Induced Phase Separation Belongs to the Ising Universality Class, *Phys. Rev. Lett.* **123**, 068002 (2019).
- [38] C. Maggi, M. Paoluzzi, A. Crisanti, E. Zaccarelli, and N. Gnan, Universality class of the motility-induced critical point in large scale off-lattice simulations of active particles, *Soft Matter* **17**, 3807 (2021).
- [39] F. Dittrich, T. Speck, and P. Virnau, Critical behavior in active lattice models of motility-induced phase separation, *Eur. Phys. J. E* **44**, 53 (2021).
- [40] T. Agranov, S. Ro, Y. Kafri, and V. Lecomte, Exact fluctuating hydrodynamics of active lattice gases—typical fluctuations, *J. Stat. Mech.* (2021) 083208.